Hydraulic and Civil Engineering Technology VII
M. Yang et al. (Eds.)

doi:10.3233/ATDE220929

Study on Deformation Characteristics and Instability Failure Mode of New Suspended Diaphragm Wall Deep Excavation in Soil-Rock Strata

Longping LI [a], Linfeng WANG [b,c1], Xiaohan ZHOU [b,c], Yunlu BAI [d] and Qiang XU [b,c]
[a] *China Railway Bridge Survey and Design Institute Group Co. LTD, Hubei 430056, P.R. China*
[b] *School of Civil Engineering, Chongqing University, Chongqing 400045, P.R. China*
[c] *Key Laboratory of New Technology for Construction of Cities in Mountain Area (Chongqing University), Ministry of Education, Chongqing 400030, P.R. China*
[d] *School of Civil, Environmental and Land Management Engineering, Politecnico di Milano, Lecco 23900, Italy*

Abstract. In the design of suspended diaphragm wall of existing soil-rock foundation pit, the bottom of the wall needs to reserve rock shoulder to provide embedding, and prestressed anchor should be used to lock the foot at the same time. It is the first time to propose a new type of suspended diaphragm wall supporting structure without rock shoulder and prestressed anchor, and makes full use of the inner struts and the middle plate of the underground structure to form a stable system, which lacks engineering experience and theoretical verification. By means of numerical simulation, the deformation characteristics and instability failure mode of soil-rock foundation pit supported by the new type of suspended diaphragm wall were discussed. The research shows that: (1) The deformation of the excavation meets the requirements under the supporting of the new suspended diaphragm wall without rock shoulder. The deformation of the wall mainly occurs in the soil section, and the deformation is mainly caused by the lateral water and soil pressure of soil. The shear stress distribution of the rock section shows that the top of the rock section is not the control point, and there is no need to take additional measures. (2) The method of ground overload can cause the damage of the supporting system components. At this time, the deformation of the rock section is still small, and the safety reserve of the rock wall section is higher than that of the supporting section. (3) By increasing the stiffness of the upper supporting structure to ensure the stability of the upper supporting structure, and increasing the ground overload to study the failure mode of the lower rock section, it is found that the failure mode of the lower rock section is that the shear stress exceeds the allowable shear strength and produces a sliding surface, and the maximum shear stress occurs at the junction of the rock section and the basement.

Keywords. Soil-rock foundation pit, new type of suspended diaphragm wall, numerical simulation, deformation characteristics, instability failure mode

[1] Linfeng Wang, Corresponding author, School of Civil Engineering, Chongqing University, Chongqing 400045, P.R. China; E-mail: 476964211@qq.com.

1. Introduction

Soil-rock foundation pit is carrying out in the strata comprised by upper soil and lower rock, which is more common as the foundation pit gets deeper (Li 2020) [1]. Soil-rock foundation pit supporting structures usually has the traditional pile anchor (strut) supporting structure form, suspended diaphragm wall (pile) anchor (strut) + bare rock supporting structure form, suspended diaphragm wall (pile) anchor (strut) + anchor spray supporting structure form and suspended diaphragm wall (pile) anchor (strut) + steel pipe pile + anchor spray supporting structure form, etc. (Ma 2012) [2]. Among them, suspended diaphragm wall (pile) supporting structure refers to the form that the retaining structure used to resist the deformation of the soil on the side of the foundation pit is only embedded in the stable rock layer and does not need to go below the bottom of the foundation pit, and has been widely used in soil-rock foundation pit (Liu et al. 2005) [3].

At present, there are abundant researches on deformation and stability of soil-rock foundation pit supported by suspended diaphragm wall. Sun et al. (2022) [4] summarized the deformation characteristics and laws of typical soil-rock foundation pit supporting structures including suspended diaphragm wall based on a soil-rock foundation pit project in Jinan. Chi et al. (2017) [5] discussed the deformation law of the soil-rock foundation pit supported by suspended diaphragm wall under asymmetrical load by means of numerical simulation. Yang (2019) [6] discussed the influence of rock-socketed depth, reserved rock shoulder width and pre-axial force of anchor cable on lateral deformation of suspended diaphragm wall. Liu (2020) [7] also carried out parameter analysis on the main influence factors of the deformation of the suspended diaphragm wall supporting structure.

In traditional suspended diaphragm wall supporting system, the rock shoulder is left at the bottom of the wall as the fixed point of the wall, and the prestressed anchor is used to lock the foot (Wu et al. 2018; Lu 2020) [8,9]. However, the reserved rock shoulder will increase the amount of excavation, enlarge the construction scope, and the prestressed anchor may affect later underground engineering. Therefore, a new type of supporting system without rock shoulder and prestressed anchor is proposed. Struts and the middle plate of the underground structure can realize the feet-lock of the wall by reasonable layout and form a stable and reliable support system together with the wall. However, due to the lack of practical engineering application, its supporting effect, deformation characteristics and failure mode are still unknown.

Therefore, based on a soil-rock foundation pit project in Guangzhou, Guangdong province, China, a numerical calculation model with the help of finite difference software FLAC^{3D}5.0 is established, the deformation law and characteristics during excavation is discussed, and the instability failure mode is summarized.

2. A New Type of Suspended Diaphragm wall Supporting Structure of Soil-rock Foundation Pit

The traditional suspended diaphragm wall supporting structure of soil-rock foundation pit needs to reserve rock shoulder at the bottom of the wall, and set the prestressed anchor bolt to lock the foot, as shown in figure 1(a). The new type of the suspended diaphragm wall supporting structure cancels the rock shoulder at the bottom of the wall, and use the last strut and middle plate of the underground structure to realize the lock-feet (figure 1(b)). The last strut provides lateral support for the bottom of the wall during excavation, and the middle plate of the underground structure is used to limit the lateral deformation on the bottom of the wall in the re-construction stage.

Compared with the traditional suspended diaphragm wall supporting structure, the advantages of this new supporting structure are as follows: (1) there is no need to excavate the rock shoulder, so it is easy for construction and saving the construction period and cost; (2) rock wall is excavated vertically and saving the amount of the excavation; (3) reducing site occupation and can construct suspended diaphragm wall according to the actual situation at any time without the need of advance planning; (4) there is no effect of feet-lock bolt on the later underground space development.

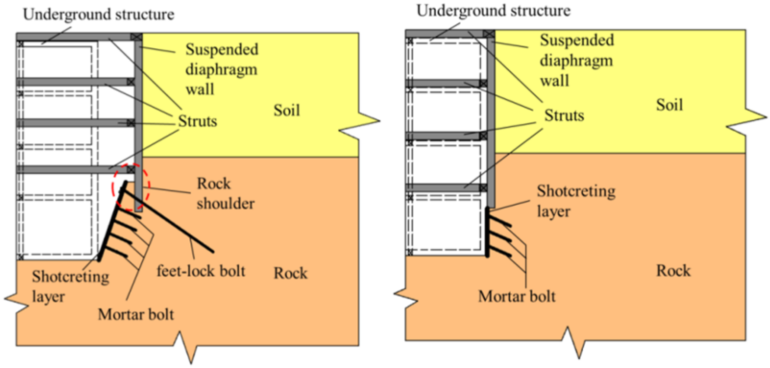

(a) Traditional suspended diaphragm wall (b) New suspended diaphragm wall

Figure 1. Traditional suspended diaphragm wall and new suspended diaphragm wall.

3. Engineering Overview and the Numerical Simulation Model

3.1. Engineering Background and Geological Conditions

The station in Guangzhou, Guangdong province, China has a total length of 276.2 m. It is a four-storey underground island station constructed by open excavation. The standard section is 47.1 m wide and 32.981 m~33.634 m deep.

The topography of the station site belongs to the alluvial plain topography of the sea-land interaction. It is a plain area with Zhujiang River. From top to bottom are miscellaneous fill, plain fill, muddy clay, fully weathered sandstone, strongly weathered sandstone, moderately weathered sandstone and slightly weathered sandstone. The distribution and thickness of each stratum are listed in figure 2. Among them, the degree of weathering of fully weathered sandstone and strongly weathered sandstone is high, which can be considered as soil layer (Shen 2018) [10]. It can be seen that the thickness of the overlying soil layer in the station site is about 19.0 m, and the station is located in the typical soil-rock strata.

3.2. Supporting Structure and Supporting Scheme

The foundation pit adopts the suspended diaphragm wall + four struts as the supporting structure. The diaphragm wall is 800 mm thick and 24.6 m deep. The bottom of the wall is located about 1.5 m below the middle plate of the negative three-layer. The four struts are all concrete struts with the depths of 0.5 m, 6.5 m, 13.8 m and 21.0 m respectively. The size of the upper three struts is 800×1000 mm, and that of the bottom strut is 1000×1300 mm. The lattice column is used to bear the struts load, and φ1500 reinforced concrete column pile is applied at the bottom of the lattice column. The base is uplifted by φ1000 reinforced concrete pile. The schematic diagram of the supporting structure is shown in figure 2. The excavation method is divided into four layers.

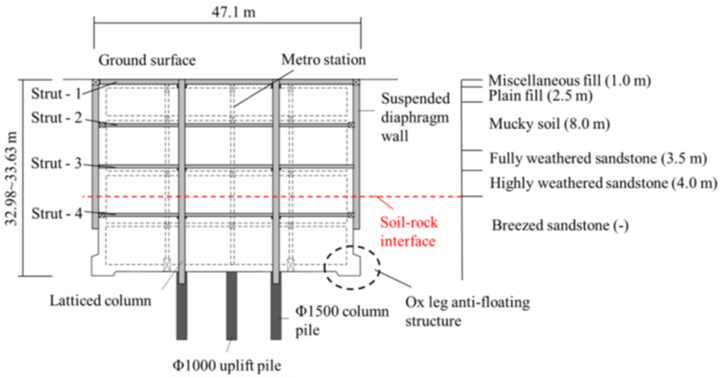

Figure 2. Typical cross section of foundation pit.

3.3. Computational Models

In order to discuss the deformation characteristics of typical soil-rock foundation pit in the whole construction process, the stratum is simplified into typical overlying soil layer and typical underlying rock layer, and the plane strain numerical calculation model is established by using finite difference software FLAC^{3D}5.0.

In the model, the foundation pit is 47.0 m long and 32.5 m deep. Considering the elimination of boundary effect, the length of the model is determined to be 249.0 m. Due to the stable bedrock under the foundation pit, 60.0 m height can meet the requirements, and the width is 1.0 m. Finally, the model size is determined to be 249.0 m × 1.0 m × 60.0 m (length × width × height), as shown in figure 3. The size and position of the supporting structure are consistent with the actual project.

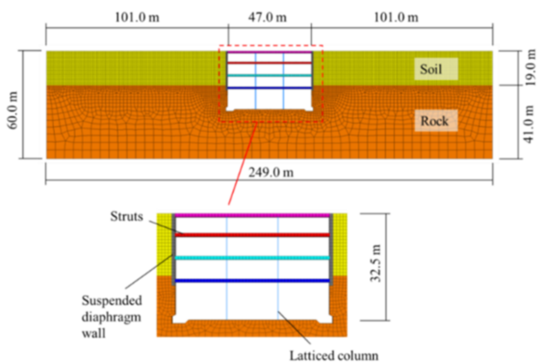

Figure 3. Numerical calculation model.

The soil layer, rock layer and suspended diaphragm wall are simulated by solid element. The latticed column, column pile and uplift pile are simulated by pile element. The strut is usually simulated by beam element. However, in this simulation, the solid element simulation is adopted to reflect the plastic failure of the strut, and the elastoplastic constitutive model is used. The boundary conditions are as follows: normal constraints are applied around the model, the bottom of the model is constrained in all directions, and the top of the model is free.

In addition, the following assumptions are made in simulation:

1) Fractures and joints in rock strata are not considered;

2) Only considers the vertical section of the excavation and neglect the step excavation under the same excavation depth;

3) Mortar bolt at the rock section in practical engineering is not considered.

3.4. Calculation Parameters

In numerical calculation, the determination of constitutive relation and parameters is very important to the calculation results. Mohr-Coulomb constitutive model is a common constitutive model in numerical simulation of underground project with the advantages of few parameters, easy obtaining, simple concept and can reflect the stress and strain characteristics of soil (Liu et al. 2022a; Liu et al. 2022b) [11,12]. Therefore, the Mohr-Coulomb constitutive model is used as the constitutive model of soil and rock in this simulation. The physical and mechanical parameters of the stratum are shown in table 1. Parameters of each layer are from the geological exploration of the excavation site.

Table 1. Physical and mechanical parameters of the strata.

Stratigraphic type	γ/(kN/m^3)	E/MPa	μ	c/kPa	φ/°	T/MPa	e	k/(m/d)
Soil	18.3	10	0.3	26.18	11.26	0.0	0.950	2.36e-12
Rock	25.6	6500	0.20	500.00	43.0	10.0	0.160	0.295e-9

In order to reflect the plastic failure of the supporting structure due to insufficient stiffness, the Mohr-Coulomb constitutive model is used in the simulation of the suspended diaphragm wall and the struts according to Sun et al. (2016) [13]. The lattice column, the column pile and the uplift pile adopt the elastic constitutive model. The specific parameters are shown in table 2.

Table 2. Supporting structure parameters.

Supporting type	γ/(kN/m^3)	E/MPa	μ	c/kPa	φ/°	T/MPa
Suspended diaphragm wall	2500	30	0.2	4070	43.87	3.5
Strut	2500	30	0.2	4070	43.87	3.5
Latticed column	7800	200	0.3	-	-	-
Erect column pile	2500	30	0.2	-	-	-
Uplift pile	2500	30	0.2	-	-	-

Interface should be set between the wall and the strata to reflect the interaction between the supporting structure and the strata. Through trial calculation, and the parameters of the contact surface are finally determined in table 3.

Table 3. Interface parameters.

Interface position	K_n/(GPa/m)	K_s/(GPa/m)	c/kPa	φ/°
Active side between wall and soil	0.1	0.1	6	14
Passive side between wall and soil	1	1	30	16
Active side between wall and rock	10	10	400	18
Passive side between wall and rock	500	500	400	26
wall bottom	500	500	400	26

3.5. Calculation process

The numerical calculation process follows the following calculation steps in table 4.

Table 4. Numerical calculation steps.

Simulation step	Simulation contents
1	Generate initial ground stress state
2	Clear the displacement and construct suspended diaphragm wall, column pile, uplift column and temporary latticed column
3	Excavate to the bottom of the first concrete strut and construct the first concrete strut (excavation step 1)
4	Dewater to -8 m, excavate to-7 m and construct the second concrete strut (excavation step 2)
5	Dewater to -15.3 m, excavate to -14.3 m and construct the third concrete strut (excavation step 3)
6	Dewater to -22.5 m, excavate to -21.5 m and construct the fourth concrete strut (excavation step 4)
7	Dewater to -34.55 m and excavate to the bottom (excavation step 5)

It should be noted that in order to accurately reflect the deformation of the foundation pit caused by the unloading of the excavation, the rebound modulus of the stratum is used instead of the elastic modulus in the excavation stage. Bi et al. (2016) [14] proposed that for foundation pit engineering, the rebound modulus of the stratum can be taken as 5 times of the elastic modulus. Therefore, the numerical simulation of this paper also takes the stratum rebound model as 5 times of the elastic modulus to participate in the calculation.

4. Deformation Characteristics

4.1. Surface Settlement

Figure 4 is the surface settlement curve outside the pit during the excavation. It can be seen that due to the shallow excavation, the surface settlement outside the pit under excavation steps 1 and 2 is basically unchanged along the distance of the pit. From excavation step 3, the surface settlement curve outside the pit begins to show a typical “groove shape”. After step 3, the maximum surface settlement increases with the excavation, and the maximum settlement position gradually moves to the outside of the foundation pit. The maximum surface settlement under the excavation steps 3,4 and 5 is about 3.5 mm, 17.5 mm and 30.5 mm, respectively. The maximum settlement positions are at 0.27H, 0.37H and 0.45H from the foundation pit (H is the depth of the foundation pit). Far away from the foundation pit, the surface is slightly uplifted, and as the excavation progresses, the uplift range gradually moves outward. In general, when the excavation is completed, the surface settlement outside the pit is in the normal range under the supporting of the new suspended diaphragm wall supporting system without rock shoulder.

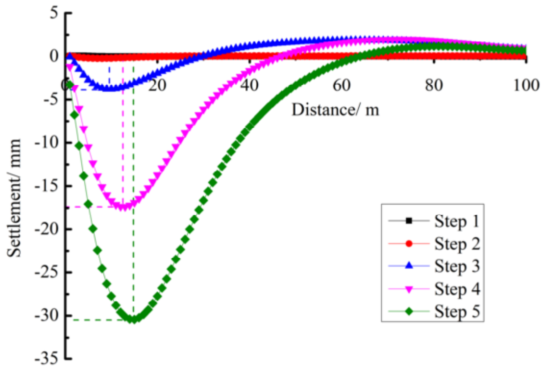

Figure 4. Ground settlement curve outside foundation pit during excavation.

4.2. Lateral Displacement of the Wall

Figure 5 is the lateral displacement curve of the suspended diaphragm wall during excavation. It can be seen that the deformation of the wall is very small under excavation step 1. In excavation step 2, the deformation of the wall begins to increase, and presents a typical “belly type”. The maximum lateral displacement reaches about 10 mm, and the maximum lateral displacement position is about 11 m. The lateral displacement of the wall gradually increases during excavation, and the maximum lateral displacement depth gradually moves down. The maximum lateral displacements under excavation steps 2-5 are about 10 mm, 15 mm, 16 mm, and 16 mm, respectively. The maximum lateral displacement depths are 11 m, 11.5 m, 12 m, and 12 m, respectively. It can be seen that the deformation of the wall mainly occurs in the excavation soil stage, and the deformation is mainly located in the soil section. From excavation of 1 m to excavation of 7 m, the maximum lateral displacement of the wall increases by about 10 mm. From excavation of 7 m to excavation of 14 m, the maximum lateral displacement of the wall increases by about 5 mm. From excavation of 14 m to excavation of 21 m, the maximum lateral displacement of the wall only increases by less than 1 mm, and then almost no longer increases. In general, the deformation of the suspended diaphragm wall meets the requirements under the supporting of the new suspended diaphragm wall supporting system without rock shoulder. In addition, the rock section is stable, and no additional measures are necessary.

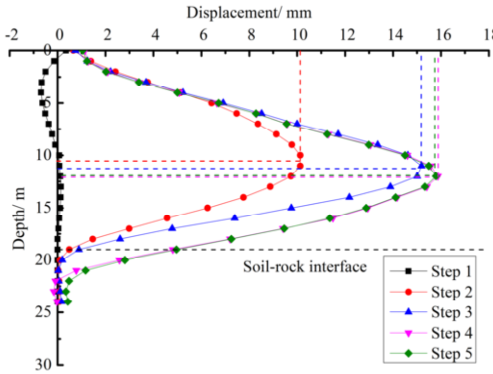

Figure 5. Lateral displacement curve of hanging wall during excavation.

5. Failure Mode

5.1. Failure Mode under Ground Overload

The above research shows that the deformation of the foundation pit meets the requirements and no instability failure will occur under the supporting of the new suspended diaphragm wall without rock shoulder and prestressed anchor cable. In order to explore the failure mode of the pit, the ground is further loaded under actual working conditions. In simulation, after the ground is loaded to 1.4 MPa, the maximum deformation of the wall exceeds 50 mm, and it is considered that the support system component is destroyed. The deformation curve of the wall along the depth is shown in figure 6. It can be seen that the maximum lateral displacement of the wall occurs at a depth of about 11 m, near the third strut between the second strut and the third strut, and at about 3/5 depth of the soil section. At the same time, the top of the wall moves about 8 mm to the inside of the pit, while the side displacement at the bottom is small, indicating that the rock section is stable due to the self-stability of the rock layer. Under the action of the last strut, it can remain stable without rock shoulder embedding. The failure of the upper soil section is the system failure caused by the failure of the supporting system components, and the soil instability failure such as kicking, overturning, and overall sliding will not occur.

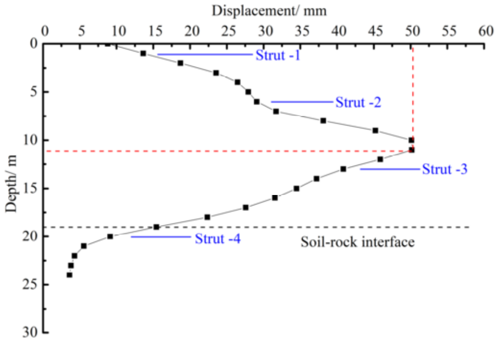

Figure 6. Deformation curve of the suspended diaphragm wall under ground overload.

Figure 7 reflects the deformation and stress of rock wall under ground overload. It can be seen that after the large deformation and instability failure of the suspended diaphragm wall, the deformation of the rock section is still small, and the maximum deformation is about 3.5 mm (figure 7 (a)). From the distribution of shear stress in the rock wall section (figure 7 (a)), it can be seen that the shear stress concentration appears at the ox leg groove due to the expansion of the excavation, and the local shear stress is about 0.89 MPa. The shear stress of the upper rock section is small, basically within 0.5 MPa. The analysis of the stress state at the ox leg groove shows that the allowable shear strength has not yet been reached. In summary, the rock section has a larger safety reserve than the upper supporting structure, and can remain stable without other engineering measures.

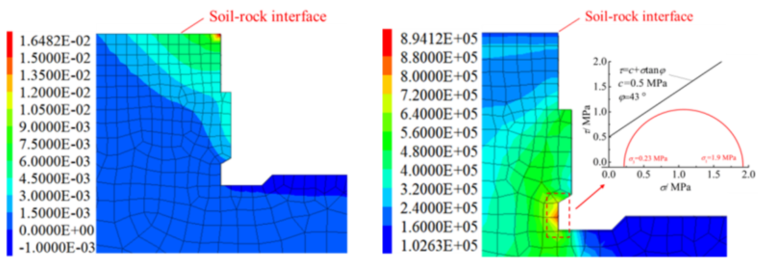

(a) Deformation of the rock section (b) Shear stress of the rock section

Figure 7. Deformation and stress of the rock section under ground overload.

5.2. Failure Mode under Ground Overload after Strengthening Supporting

The study in the previous section found that through the way of ground overload, the large deformation instability of the supporting system in the upper soil layer is finally presented, while the rock section is still in a stable state. In order to further explore the instability failure mode of the rock section, the stiffness of the upper supporting structure is increased and the ground is overloaded in this section. In the simulation, the stiffness of the supporting structure is increased by 10 times. After the ground is loaded to 3.6 MPa, the rock wall is destabilized and destroyed. The main manifestation is that the shear stress exceeds the allowable shear strength and produces a sliding surface from the soil-rock interface to the basement. At this time, the maximum lateral displacement of the wall is about 9 mm, which achieves the effect of stabilizing the upper soil layer by increasing the stiffness of the supporting structure.

Figure 8 is the deformation of the rock section under ground overload after strengthening supporting. At this time, the maximum deformation of the rock section is nearly 8 mm, and the deformation is still not large. From the maximum shear strain increment cloud map of the rock section (figure 9 (a)), it can be seen that there is a linear sliding surface-1 from the ox leg groove in the rock section oblique to the soil-rock interface. At the same time, there is also an arc sliding surface-2 along the bottom of the wall to the ox leg groove. The principal stress of the rock section is extracted and compared with the allowable value of the shear strength of the rock material to analyze whether there is shear failure in the rock section. It is found that the ox leg groove is the most unfavorable position, where the Mohr circle has been tangent to the shear strength envelope of the rock material, indicating that the shear failure has occurred (figure 9 (b)). All signs show that the foundation pit has been destabilized at this time, and the instability failure is characterized by the shear failure of the lower rock section.

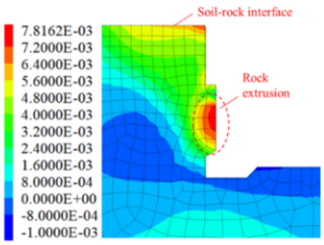

Figure 8. Deformation of the rock section under ground overload after strengthening supporting.

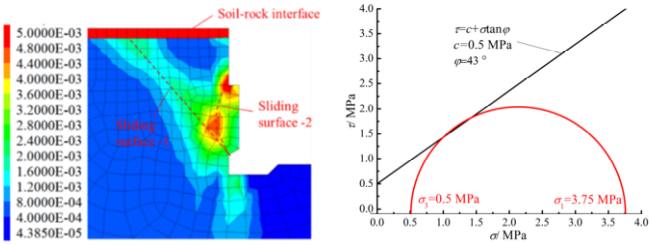

(a) Maximum shear strain increment; (b) The Mohr circle of the most unfavorable position

Figure 9. Rock section instability determination under ground overload after strengthening supporting.

6. Conclusion

The finite difference software FLAC^{3D}5.0 is used to establish the numerical calculation model. The deformation law and characteristics of soil-rock foundation pit under the support of a new type of suspended diaphragm wall supporting structure are discussed, and the instability failure mode is summarized. The conclusion is as follows:

(1) Under the actual working conditions, the surface settlement curve outside the pit shows a typical “groove shape” law, and the deformation of the suspended diaphragm wall shows a typical “belly type” law. The deformation of the pit meets the requirements. The deformation of the wall mainly occurs in the soil section, and is mainly caused by the lateral water and soil pressure. The shear stress distribution of the rock section shows that the top of the rock section is not the control point, and it is not necessary to take additional measures.

(2) The method of ground overload can cause the damage of the supporting system components, and there will be no soil instability damage such as kicking, overturning, and overall sliding. The deformation of the rock section is still small, and the safety reserve of the rock section is higher than that of the supporting section.

(3) By increasing the stiffness of the upper supporting structure to ensure its stability, and increasing the ground overload to study the failure mode of the lower rock section. It is found that the failure mode of the lower rock section is that the shear stress exceeds the allowable shear strength and produces a sliding surface, and the maximum shear stress occurs at the junction of the rock section and the basement.

Acknowledgements

The study is supported by Graduate Scientific Research and Innovation Foundation of Chongqing, China (Grant No. CYB20031).

References

[1] Li HX. Research on deformation regularity and stability of “end-hanging pile” support system for deep foundation in earth-rock stratum. Guang Zhou: Guang Zhou University, 2020. (in Chinese)
[2] Ma L. Discussion on various support form in "dual structure of soil and rock. Value Engineering. 2012; 31(9): 87. (in Chinese)
[3] Liu TJ, Mo HH, Chen JS. Feasibility analysis of a no-changing-support construction plan of the foundation pit project. Construction Technology. 2005; (6): 42-44. (in Chinese)
[4] Sun LY, Duan SQ, Li MY, et al. Study on deformation characteristics of deep foundation excavation in strata with soil-rock combination in Jinan. Construction Technology, 2022, 51(13): 13-20. (in Chinese)
[5] Chi XW, Chen ZF. Deformation analysis for the end-suspended piles in deep foundation pits with asymmetric soil-rock strata. Construction Technology. 2017; 46(S1): 84-87. (in Chinese)
[6] Yang JH. Numerical analysis on design of soil-rock dualistic foundation pit with end-suspended piles. Fujian Construction Science & Technology. 2019; (4): 32-35. (in Chinese)
[7] Liu MZ. Research on the application of “end-suspended pile” in soil-rock combination foundation pit. Baoding: Hebei Agricultural University, 2020. (in Chinese)
[8] Wu J, Yang ZY, Liao SM, et al. Mechanical analysis and design optimization of end-suspended piles of deep foundation pit in soil-rock composite strata. Tunnel Construction. 2018; 38(S2): 80-86. (in Chinese)
[9] Lu T. Deformation characteristics analysis and optimization design of rock-soil combination foundation pit in Jinan area. Jinan: Shandong University, 2020. (in Chinese)
[10] Shen YS. Study on deformation characteristics and control indexes of deep foundation pit of soil-rock combined subway. Zhenjiang: Jiangsu University Press, 2018. (in Chinese)
[11] Liu XR, Wang LF, Zhou XH, et al. E-M calculation model and its application of calculating deformation in a new tunnel orthogonally undercrossing an existing tunnel. Tunnelling and Underground Space Technology. 2022a; 123: 104418.
[12] Liu XR, Liu DS, Xiong F, et al. Experimental and numerical study on the stability of slurry shield tunneling in circular-gravel layer with different cover-span ratios. Geomechanics and Engineering, 2022b; 28(3): 265-281.

[13] Sun Y, Zhang DL, Yu FC, et al. Deformation characteristics and ultimate bearing capacity of secondary lining for high speed railway tunnel. China Railway Science. 2016; 37(1): 60-70. (in Chinese)
[14] Bi G, Wei JF, Niu HM. The realization of soil rebound deformation based on FLAC3D. China Water Transport. 2016; 16(7): 305-307, 309. (in Chinese)